Solitary water wave interactions

By Walter Craig

Department of Mathematics and Statistics
McMaster University
Hamilton, Ontario L8S 4K1, Canada
`http://www.math.mcmaster.ca/ craig`

Our concern in this talk is the problem of free surface water waves, the form of solitary wave solutions, and their behavior under collisions. Solitary waves for the Euler equations have been described since the time of Stokes. In a long wave perturbation regime they are well described by single soliton solutions of the Korteweg deVries equation (KdV). It is a famous result that multiple soliton solutions of the KdV exhibit elastic collisions. The question is as to what extent interactions between Stokes solitary waves deviate from being elastic. In this talk I will present numerical, experimental and analytical results on this question, concerning both co-propagating and counter-propagating cases of large amplitude solitary waves. In all cases we find evidence of inelastic interactions, but it is remarkable to me how collisions of even large solitary waves are very close to being elastic, and how small is the residual. This work is the result of a collaboration with P. Guyenne (Delaware), J. Hammack and D. Henderson (PSU), and C. Sulem (Toronto), which appears in the paper [4].

Keywords: Solitary waves, nonlinear wave interactions

1. Equations of motion for potential flow

The presentation is a discussion of the classical problem of interactions between solitary water waves. There are two basic cases; the interaction between counter-propagating waves (either symmetric collisions or collisions between waves of different amplitudes), and co-propagating or overtaking interactions. This work updates the well-known numerical simulations of Chen and Street [2], Fenton and Reinecker [7], and Cooker, Weidman and Bale [3]. It has also been compared with the experimental results of Maxworthy [10] and our own experiments [4]. We work with potential flow, for which the velocity potential satisfies

$$\Delta\varphi = 0\,, \tag{1.1}$$

in the fluid domain. It is bounded below by $\{y = -h\}$, while the free surface is given in the form of a graph $\{y = \eta(x,t)\}$. On the bottom boundary of the fluid domain we impose

$$N \cdot \nabla\varphi = 0 \quad \text{on} \quad y = -h\,, \tag{1.2}$$

and on the free surface we impose the two classical boundary conditions

$$\left.\begin{aligned} \partial_t\varphi + \tfrac{1}{2}|\nabla\varphi|^2 + g\eta = 0 \\ \partial_t\eta + \partial_x\eta\cdot\partial_x\varphi - \partial_y\varphi = 0 \end{aligned}\right\} \quad \text{on} \quad y = \eta(x,t)\,, \tag{1.3}$$

These equations can be posed in the form of a Hamilton system, a fact which is due to V.E. Zakharov [13]. Zakharov's Hamiltonian can be rewritten [6] as

$$H(\eta,\xi) = \tfrac{1}{2}\int_{-\infty}^{\infty} \xi G(\eta)\xi + g\eta^2 \, dx \ . \tag{1.4}$$

In this expression we write $\xi(x) := \varphi(x,\eta(x))$, and the Dirichlet integral, which represents the kinetic energy, is expressed in terms of the Dirichlet − Neumann operator

$$G(\eta)\xi := \sqrt{1+|\partial_x\eta|^2}\; N\cdot\nabla\varphi\Big|_{y=\eta} \ , \tag{1.5}$$

The equations (1.1) through (1.3) are written in the canonical form

$$\partial_t \begin{pmatrix}\eta\\ \xi\end{pmatrix} = \begin{pmatrix}0 & 1\\ -1 & 0\end{pmatrix}\begin{pmatrix}\delta_\eta H\\ \delta_\xi H\end{pmatrix} \ . \tag{1.6}$$

Explicitely, Hamilton's canonical equations (1.6) have the form

$$\partial_t\eta \;=\; G(\eta)\xi \, , \tag{1.7}$$

$$\partial_t\xi \;=\; -g\eta + \frac{-1}{2(1+|\partial_x\eta|^2)}\left[(\partial_x\xi)^2 - (G(\eta)\xi)^2 - 2\partial_x\eta\partial_x\xi\, G(\eta)\xi\right] \ . \tag{1.8}$$

The second component (1.8) of this Hamiltonian vector field has an additional term in the case of the water wave equations in three dimensions.

The time evolution of (1.6) conserves a number of physical quantities in addition to the Hamiltonian, including the *added mass*

$$M(\eta) = \int_{-\infty}^{\infty} \eta(x,t)\, dx \tag{1.9}$$

and the momentum, or *impulse*

$$I(\eta,\xi) = \int_{-\infty}^{\infty} \eta(x,t)\partial_x\xi(x,t)\, dx \ . \tag{1.10}$$

This is verified by the following identities

$$\{M,H\} = 0 \quad , \qquad \{I,H\} = 0 \ , \tag{1.11}$$

where the *Poisson bracket* between two functionals F and H is given by

$$\{F,H\} = \int \delta_\eta F \delta_\xi H - \delta_\xi F \delta_\eta H \, dx \ . \tag{1.12}$$

The *center of mass* of a solution is given by the expression

$$C(\eta) = \int_{-\infty}^{\infty} x\eta(x,t)\, dx \ . \tag{1.13}$$

It evolves linearly in time; indeed its time derivative is a constant of motion

$$\begin{aligned} \frac{d}{dt}C &= \int_{-\infty}^{\infty} x\partial_t\eta(x,t)\, dx = \int_{-\infty}^{\infty} xG(\eta)\xi\, dx \\ &= \int_{-\infty}^{\infty} \xi G(\eta)x\, dx = \int_{-\infty}^{\infty} \xi(-\partial_x\eta)\, dx = I(\eta,\xi) \ . \end{aligned} \tag{1.14}$$

2. Numerical method

Our numerical method consists essentially in making good approximations for the Dirichlet – Neumann operator (1.5), and using them in a time discretized version of the evolution equations (1.7). This approach was introduced in [6] and used in a variety of settings, including [5][1].

It was already described by J. Hadamard [8] in his Collège de France lectures that Green's function for Laplace's equation is differentiable with respect to the domain on which it is given. Indeed he gave a formula for its variations, and in [9] he proposed hydrodynamical applications. In fact in the appropriate setting it has been shown that the closely related Dirichlet – Neumann operator is analytic with respect to its dependence upon the domain. Putting this into practice in the neighborhood of a fluid domain at rest, we base our simulations on the Taylor expansion of the Dirichlet – Neumann operator to arbitrarily high order in the equations of motion (1.7). The first several Taylor approximations to $G(\eta)$ are

$$\begin{aligned} G^{(0)} &= D\tanh(hD)\,, \\ G^{(1)} &= D\eta D - G^{(0)}\eta G^{(0)}\,, \\ G^{(2)} &= \tfrac{1}{2}\left(G^{(0)}D\eta^2 D - D^2\eta^2 G^{(0)} - 2G^{(0)}\eta G^{(1)}\right)\,. \end{aligned} \tag{2.1}$$

In our notation, $D = -i\partial_x$, and $G^{(0)}$ is a Fourier multiplier operator which is given by the expression

$$G^{(0)}\xi(x) := \frac{1}{\sqrt{2\pi}}\int e^{ikx}k\tanh(hk)\hat{\xi}(k)\,dk \tag{2.2}$$

Such expressions can be implemented efficiently using the Fast Fourier Transform. As well, there is a recursion formula for the Taylor series for $G(\eta)$ which can be incorporated into very efficient numerical schemes of arbitrarily high order in the (slope of the) surface elevation $\eta(x)$. This is essentially what we have done in [4] for our study of solitary water wave interactions.

Initial data for our simulations consists of two well separated solitary water waves, of nondimensional amplitudes S_1/h and S_2/h, which are set to collide within the computational domain. The solitary wave profiles for this are generated using the numerical method proposed by M. Tanaka [12], giving us highly accurate results.

3. Head-on collisions

This section is concerned with collisions between two counter-propagating solitary waves, of nondimensional elevation S_1/h and S_2/h respectively. The first simulations presented here are symmetric head-on collisions between two solitary waves of equal amplitudes S/h. Features of note are the degree of *run-up* of the wave crest during the interaction, given by $\sup_{x,t}|\eta(x,t)|/h - 2S/h$; the phase lag due to the moment's hesitation of the crests during their interaction; the change in amplitude of the solitary waves after the interaction, $S/h \mapsto S^+/h$; their phase lag $a \mapsto a^+$; and the *residual* waves $\eta_R(x,t)$ trailing the solitary waves as they exit the collision. We observe that the solitary waves in head-on collisions always lose a small amount of amplitude due to the collision; $S_j^+ < S_j$, although this is very small even for interactions between large solitary waves.

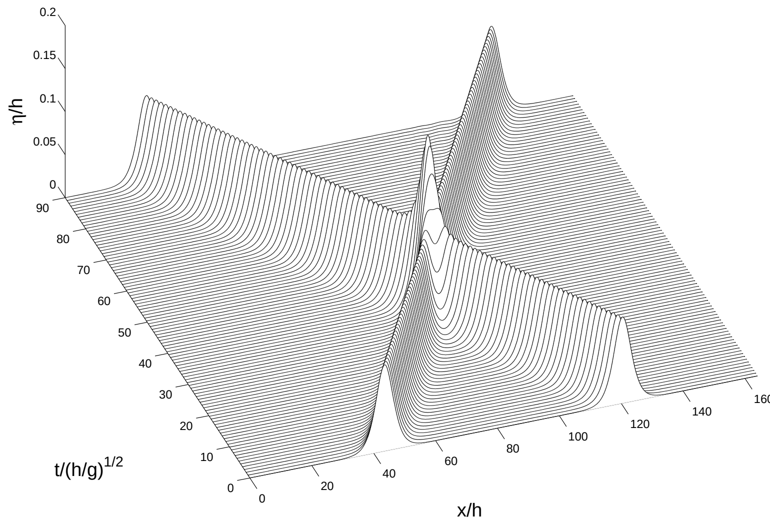

Figure 1. Head-on collision of two solitary waves of equal height $S/h = 0.1$: The amplitude after collision is $S^+/h = 0.0997$ at $t/\sqrt{h/g} = 90$. The phase lag is $(a_j - a_j^+)/h = 0.1370$.

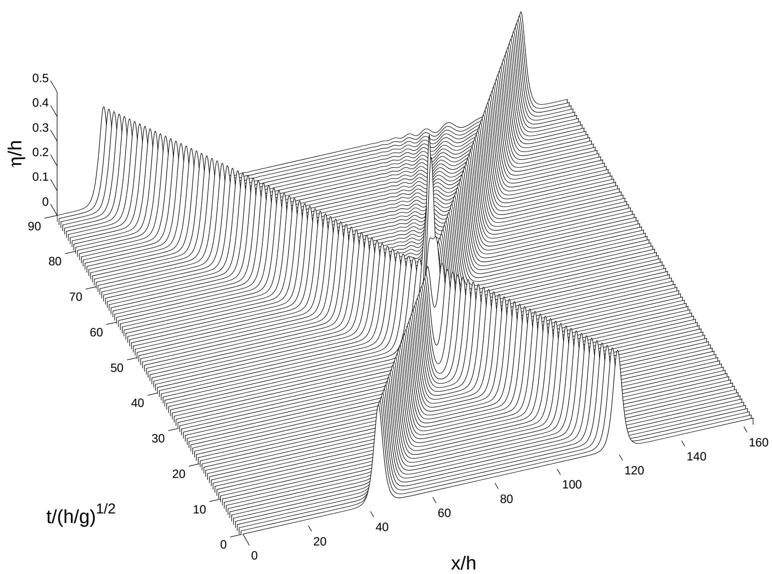

Figure 2. Head-on collision of two solitary waves of equal height $S/h = 0.4$: The amplitude after collision is $S^+/h = 0.3976$ at $t/\sqrt{h/g} = 90$. The phase lag is $(a_j - a_j^+)/h = 0.3257$.

The residual is clearly visible in the figure 2, but it is essentially too small to be detected in figure 1 without magnification. A snapshot plot of the computation in figure 1 at time $t/\sqrt{h/g} = 90$, with magnified vertical scale, is given in the figure 3.

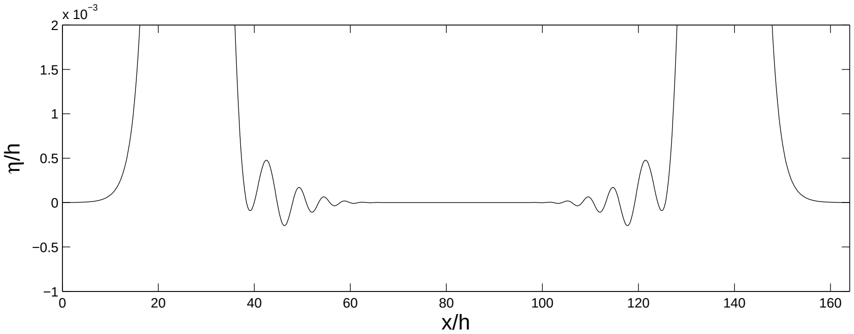

Figure 3. Results of the collision of two solitary waves of equal height $S/h = 0.1$ after the collision, at time $t/\sqrt{h/g} = 90$. The dispersive residual wave trailing the solitary waves after the collision are visible under magnification.

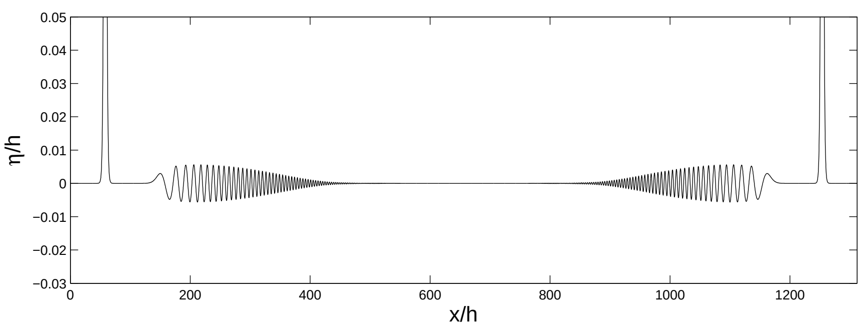

Figure 4. Results of the collision of two solitary waves of equal height $S/h = 0.4$ after the collision at time $t/\sqrt{h/g} = 780$. The residual has a characteristic tear-shaped envelope

Viewing the interaction of two solitary waves of amplitude $S/h = 0.4$ after long time illustrates the asymptotic tear-shaped form of the residual, as well as the fact that the solitary waves separate from each other *and* from the the residual after the collision. This is shown in figure 4; it is an indication of the stability of solitary waves to such head-on collisions, at least within this range of amplitudes.

4. Overtaking collisions

We have also run simulations of overtaking collisions with this numerical scheme, where we find yet smaller changes of amplitude $\Delta S_j := S_j - S_j^+$, $j = 1, 2$ and residual η_R after a collision. Normalize the notation so that the larger incoming solitary wave has amplitude S_1 and the second S_2. In these simulations, we observe that the amplitude of the first solitary wave is slightly *increased*, $S_1^+ > S_1$, while the second decreases as is necessary. We also observe that the amplitude of the solution never exceeds the maximum of the amplitudes of the entering and exiting solitary waves, nor at any time does the maximum crest dip below the minimum. Just as in the situation of the two-soliton solution of the KdV equation, the solitary waves experience a positive phase shift due to the collision, as though the two waves were repelling particles. Figure 5 shows the interaction of two solitary waves of amplitudes $S_1/h = 0.4$ and $S_2/h = 0.1333$, this being chosen so that the interaction

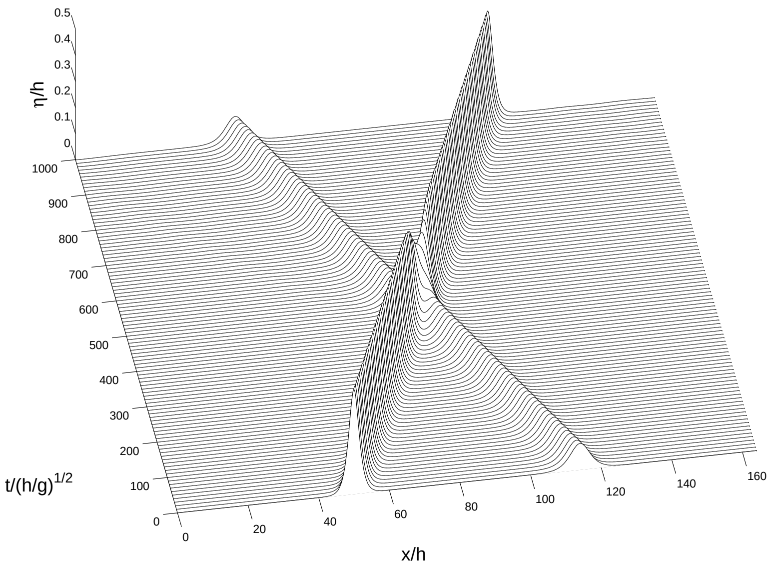

Figure 5. Overtaking collision of two solitary waves of height $S_1/h = 0.4$, $S_2/h = 0.1$: The amplitudes after collision are $S_1^+/h = 0.4003$, $S_2^+/h = 0.0999$ at $t/\sqrt{h/g} = 1000$ for the large, small wave respectively. The phase shifts are $(a_1^+ - a_1)/h = 2.2974$, $(a_2^+ - a_2)/h = 3.6159$ respectively.

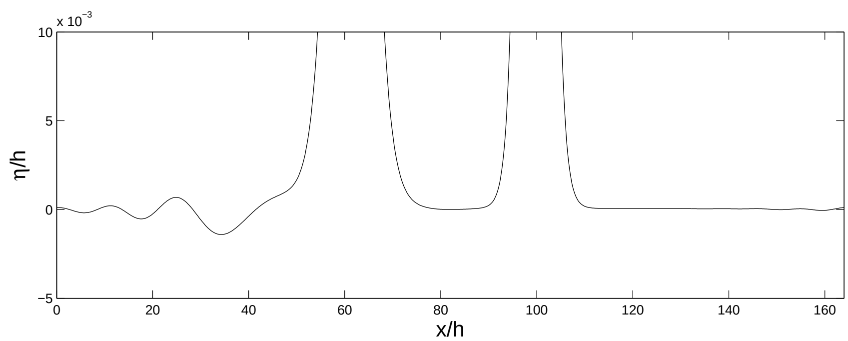

Figure 6. Overtaking collision of two solitary waves of height $S_1/h = 0.4$, $S_2/h = 0.1$ at $t/\sqrt{h/g} = 745$, which is after the collision. The vertical scale is magnified in order to observe the dispersive trailing wave generated by the interaction.

is of the Lax category (b) in its form. The simulation is displayed in a frame of reference in motion at approximately the mean velocity of the two solitary waves.

In figure 6 a view of this simulation with exagerated scale at a time after the interaction shown clearly the very small but nonzero residual.

5. Energy transfer

Using the conservation laws (1.9)(1.10) and the Hamiltonian (1.4), one can derive a relation between the change in amplitude through a solitary wave interaction and the energy that has been transferred to the residual. Using this, it is also possible to derive a rigorous upper bound on the energy transfer in terms of the parameters $S_1/h, S_2/h$ of the initial data. The latter analysis appears in [4]. To explain the first relation, an individual solitary wave has mass $M(\eta_S) := m(S)$, momentum $I(\eta_S, \xi_S) := \mu(S)$ and energy $H(\eta_S, \xi_S) := e(S)$. Our initial data is given by two asymptotically separated solitary waves as $t \mapsto -\infty$, therefore the total mass, momentum and energy of our solution are given by

$$\begin{aligned} M_T &= m(S_1) + m(S_2) \\ I_T &= \mu(S_1) + \mu(S_2) \\ E_T &= e(S_1) + e(S_2) \ . \end{aligned} \tag{5.1}$$

After an interaction has occurred, we will assume that the solution is composed of three distinct components; two solitary waves with possibly different amplitudes S_1^+ and S_2^+, and a residual $(\eta_R(x,t), \xi_R(x,t))$. By conservation, their mass, momenta and energies satisfy

$$\begin{aligned} M_T &= m(S_1^+) + m(S_2^+) + m_R \\ I_T &= \mu(S_1^+) + \mu(S_2^+) + \mu_R \\ E_T &= e(S_1^+) + e(S_2^+) + e_R \ . \end{aligned} \tag{5.2}$$

Taking the difference, we find that

$$\begin{aligned} (m(S_1) - m(S_1^+)) + (m(S_2) - m(S_2^+)) &= m_R \\ (\mu(S_1) - \mu(S_1^+)) + (\mu(S_2) - \mu(S_2^+)) &= \mu_R \\ (e(S_1) - e(S_1^+)) + (e(S_2) - e(S_2^+)) &= e_R \ . \end{aligned} \tag{5.3}$$

Since the change in amplitude is very small, the difference $m(S_j) - m(S_j^+)$ is very small, $j = 1, 2$, and the same for $\mu(S_j)$ and $e(S_j)$. Approximating by the derivative, we conclude that

$$\begin{aligned} m_1' \Delta S_1 + m_2' \Delta S_2 &= m_R \\ \mu_1' \Delta S_1 + \mu_2' \Delta S_2 &= \mu_R \\ e_1' \Delta S_1 + e_2' \Delta S_2 &= e_R \ ; \end{aligned} \tag{5.4}$$

this is now three equations for the two unknowns Δ_j, $j = 1, 2$, whose solution leads us to an absolute bound on the energy loss due to a collision [4]. Separately from this bound, equations (5.4) specify relationships between the mass, momentum and energy loss to the residual and the change in amplitude ΔS_j from the interaction.

Let us consider the case of symmetric interactions as an example. In this case, $\mu(S_1) = -\mu(S_2)$ and therefore $I_T = 0$ and $\mu_R = 0$. The relation (5.4) then reports that

$$2m'(S) = m_R \ , \qquad 2e'(S) = e_R \ . \tag{5.5}$$

Since in particular $e(S) \sim S^{3/2}$ for small S, this predicts that

$$e_R \sim S^{1/2} \Delta S \ . \tag{5.6}$$

Figure 7 plots the quantity $e(S)$ for a range of simulations ranging from $S = 0.025$ to $S = 0.5$, verifying its power law behavior. Figure 8 gives our measured values

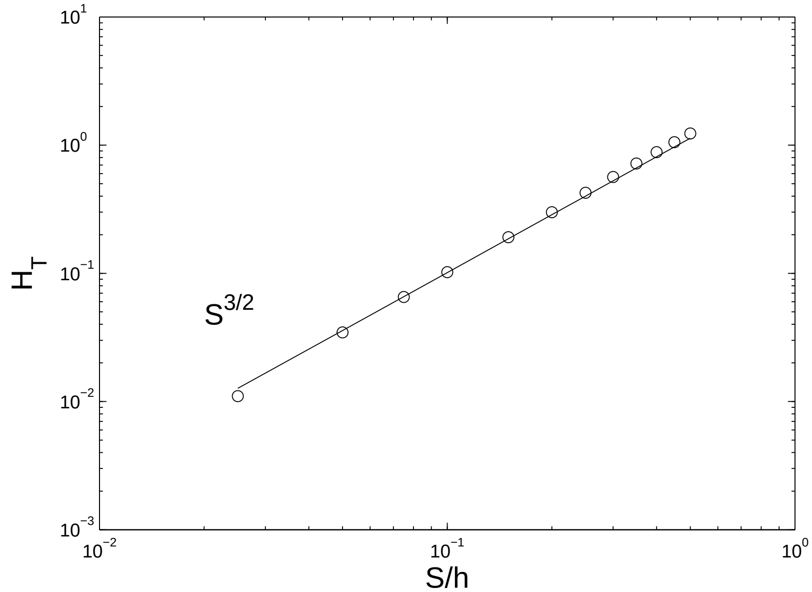

Figure 7. Total energy E_T vs. wave amplitude S/h: numerical results (circles), power law $(S/h)^{3/2}$ (solid line).

of ΔS for these simulations, while figure 9 gives the energy e_R of the residual. The adherence of thie data to the asymptotic relation (5.6) is quite convincing. The deviation of the lowest two data points from the power law behavior is due to the long relaxation time of small solutions to their asymptotic values after an interaction, we believe.

Our data, particularly in figure 8, are at odds with the asymptotic predictions of C.-H. Su and R. M. Mirie [11], who put forward that $\eta_R = \mathcal{O}(S^3)$ while $\Delta S = o(S^3)$.

The relations (5.4) give a nontrivial result on the mass and energy of the residual and the quantities ΔS_j^+ in the case of overtaking collisions. From our simulations and from those in [7], it is observed that $\Delta S_1 < 0$. That is, the larger overtaking solitary wave gains a (small amount of) amplitude due to the collision, at the expense of the smaller one. We note that $e(S)$ is a convex function of S, at least over the range of values of S being considered. The implication of (5.4) is that, since $e_R \geq 0$, it must be that $|\Delta S_1| < \Delta S_2$; the larger solitary wave cannot gain more amplitude than the smaller one loses. Using this, a related argument applied to the relation for mass implies that $m_R < 0$, because in this case $m'(S)$ is decreasing in S. This fact is seen in the slight depression left behind two separating solitary waves after their interaction.

Acknowledgements: This research has been supported in part by the Canada Research Chairs Program, the NSERC under operating grant #238452, and the NSF under grant #DMS-0070218. All of the numerical simulations in this note were performed by P. Guyenne.

References

[1] W. J. D. Bateman, C. Swan and P. Taylor. On the efficient numerical simulation of directionally spread surface water waves. *J. Comput. Phys.* **174**, 277 (2001).

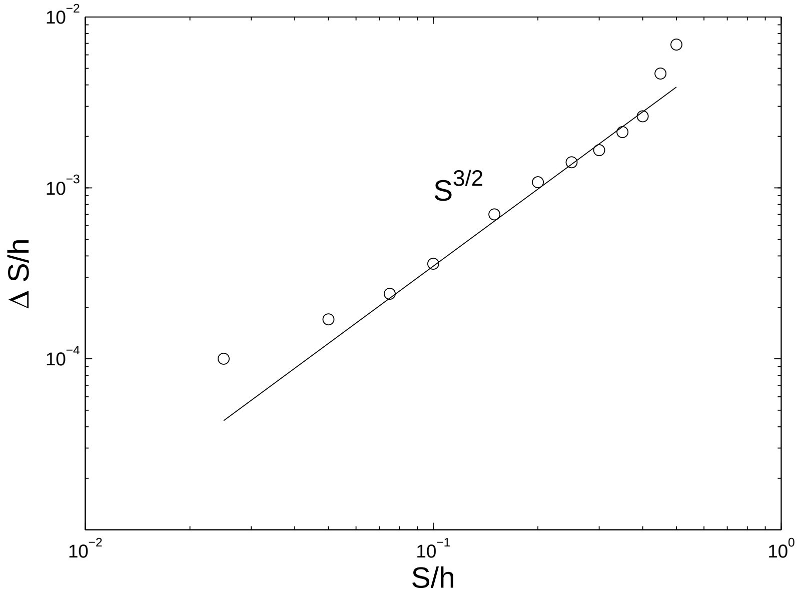

Figure 8. Change in amplitude $\Delta S/h = (S - S^{+})/h$ vs. wave amplitude S/h: numerical results (circles), power law $(S/h)^{3/2}$ (solid line).

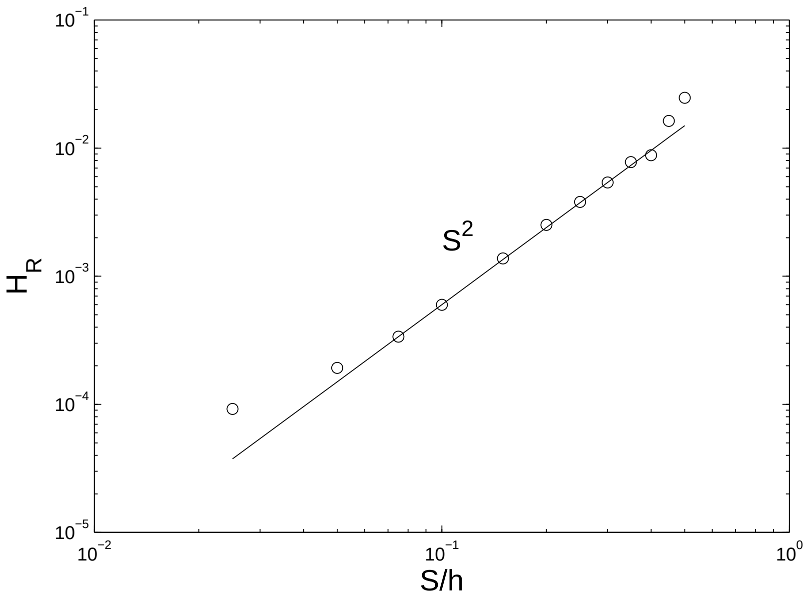

Figure 9. Energy of the residual e_R vs. nondimensional wave amplitude S/h: numerical results (circles), power law $(S/h)^2$ (solid line).

[2] R. K.-C. Chan, and R. Street. A computer study of finite amplitude water waves. *J. Comput. Phys.* **6**, 68 (1970).

[3] M. J. Cooker, P. D. Weidman, and D. S. Bale. Reflection of a high-amplitude solitary wave at a vertical wall. *J. Fluid Mech.* **342**, 141 (1997).

[4] W. Craig, P. Guyenne, J. Hammack, D. Henderson and C. Sulem. Solitary wave interactions. *Physics of Fluids* (2005), submitted.

[5] W. Craig & D. Nicholls. Traveling two and three dimensional capillary gravity waves. *SIAM: Math. Analysis* **32** (2000), pp. 323-359.

[6] W. Craig and C. Sulem. Numerical simulation of gravity waves. *J. Comp. Phys.***108**, pp. 73–83, (1993).

[7] J. D. Fenton, and M. M. Rienecker. A Fourier method for solving nonlinear water-wave problems: application to solitary-wave interactions. *J. Fluid Mech.* **118**, 411 (1982).

[8] J. Hadamard. *Leçons sur le calcul des variations*. Hermann, Paris, 1910; paragraph §249.

[9] J. Hadamard. Sur les ondes liquides. *Rend. Acad. Lincei* **5**, (1916) no. 25, pp. 716–719.

[10] T. Maxworthy. Experiments on the collision between two solitary waves. *J. Fluid Mech.* **76**, 177 (1976).

[11] C. H. Su, and R. M. Mirie. On head-on collisions between two solitary waves. *J. Fluid Mech.* **98**, 509 (1980).

[12] M. Tanaka. The stability of solitary waves. *Phys. Fluids* **29**, 650 (1986).

[13] V.E. Zakharov. Stability of periodic waves of finite amplitude on the surface of a deep fluid. *J. Appl. Mech. Tech. Phys.* **9** (1968), pp. 190–194.